

Article

Study on the Migration Law of Dissolved Organic Matter in Mine Water Treatment Station

Xiyu Zhang ^{1,2,3,*}, Shuning Dong ^{2,3}, Pengkang Jin ¹, Jidong Liang ¹, Jian Yang ^{2,3} and Yongan Huang ⁴¹ School of Energy and Power Engineering, Xi'an Jiaotong University, Xi'an 710049, China² CCTEG Xi'an Research Institute, Xi'an 710054, China³ Shaanxi Engineering Research Center of Mine Ecological Environment Protection and Restoration in the Middle of Yellow River Basin, Xi'an 710054, China⁴ Shaanxi Coal Industry Yubei Coal Industry Co., Ltd., Yulin 719000, China

* Correspondence: zhangxiyu@cctegxian.com

Abstract: With the improvement of coal-mining mechanizations and the intensification of human activities, the organic matter pollution of mine water is becoming severe. In this study, the chemical compositions of the influents and effluents from 15 mine water treatment stations in the mining area bordering Mongolia and Shaanxi were measured. The occurrence of DOM (dissolved organic matter) in the effluent from the mine water treatment stations in this area was determined by the EEM (excitation emission matrix), combined with the PARAFAC (parallel factor analysis) method. The DOM removal from the mine water treatment station in the Caojiatan coal mine is specifically discussed here, although trends are similar across the 15 mines. The treatment capacity of this treatment process for different types of pollutants is also evaluated, and a mine water treatment process suitable for the current coal-mining mode is suggested. The results show that the DOM of the mine water treatment stations in this area mainly has four components: a fulvic-acid-like substance (C1/C3), a protein tryptophan-like substance (C2), and a protein tyrosine-like substance (C4). The coagulation, filtration, and disinfection process has a removal efficiency of more than 90% for the protein-like tryptophan components, COD (chemical oxygen demand), and NO_2^- , and an efficiency of ~50% for TOC (total organic carbon), <30% for Cu^{2+} and F^- , and almost no removal effect for protein-like tyrosine components, EC (electrical conductivity), TDS (total dissolved solids), and NH_4^+ . These conclusions show that aliphatic hydrocarbons, such as alkanes and cycloalkanes, in mine water are removed by the treatment process, whereas macromolecular aromatic hydrocarbons and other groups are not removed by the treatment process. Based on this, an ozone-demulsification process for the special removal of protein tyrosine-like pollutants in mine water is proposed. This conclusion can provide theoretical support for research on the source and fate of the carbon trajectory in the water-cycle process and provides technical guidance for the removal of DOM from mine water.

Keywords: mine water; DOM; parallel factor; EEM; ozone demulsification

Citation: Zhang, X.; Dong, S.; Jin, P.; Liang, J.; Yang, J.; Huang, Y. Study on the Migration Law of Dissolved Organic Matter in Mine Water Treatment Station. *Water* **2022**, *14*, 3339. <https://doi.org/10.3390/w14203339>

Academic Editor: Liliana Letticariu

Received: 13 September 2022

Accepted: 18 October 2022

Published: 21 October 2022

Publisher's Note: MDPI stays neutral with regard to jurisdictional claims in published maps and institutional affiliations.



Copyright: © 2022 by the authors. Licensee MDPI, Basel, Switzerland. This article is an open access article distributed under the terms and conditions of the Creative Commons Attribution (CC BY) license (<https://creativecommons.org/licenses/by/4.0/>).

1. Introduction

DOM is the general term for dissolved organic material in water [1]. As the world's largest organic carbon pool, the DOM cycle in aquatic environments occurs through soil, rivers, and other media via the actions of water itself and other geological forces to maintain the balance of the water ecosystem [2]. In recent years, China's rapid industrial activities and urbanization processes have greatly impacted the water ecosystem [3], increasing the severity of DOM pollution in water bodies. An increase in the degree of mine mechanization promotes the progress of the coal industry, but high-intensity mining is associated with a series of ecological problems, such as surface subsidence and water damage. Coal mine drainage is a kind of water resource that will seep from the aquifer into the underground coal mine during coal mine production. The DOM flows into mine drainage along with water body, which includes hydrophilic organic acids, carbohydrates, and protein-like,

amino-acid-like, and hummus-like substances [4] that originate from either endogenous (internal) or exogenous (external) sources (Figure 1).

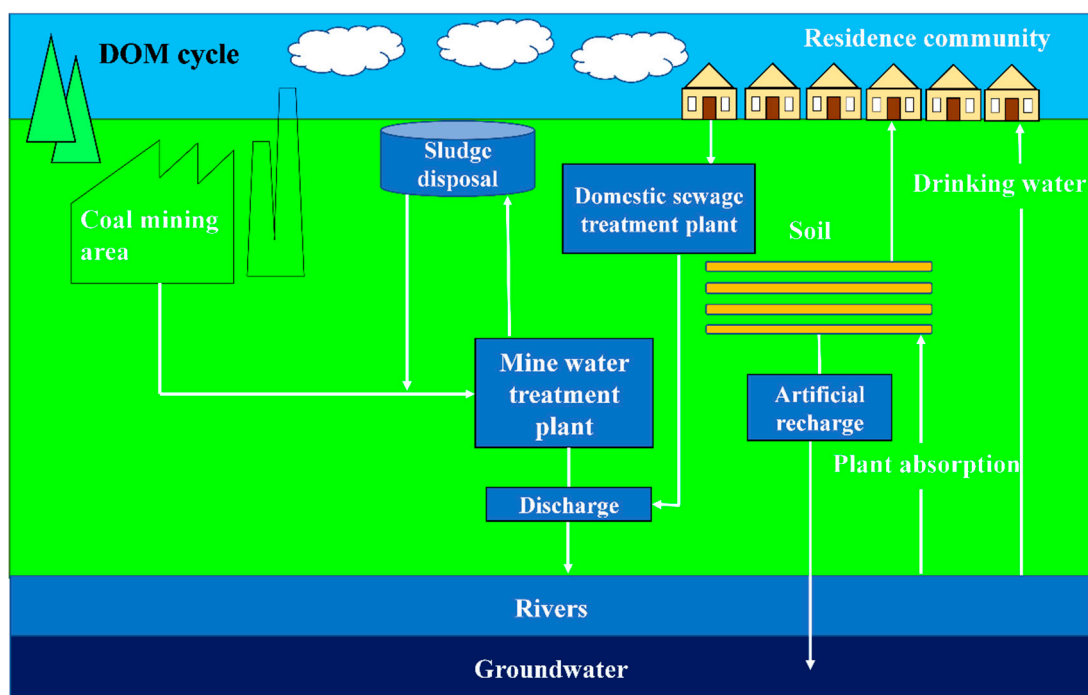


Figure 1. Schematic diagram of the DOM cycle in a coal mine area.

Studies have shown that most of the DOM in mine water comes from emulsified oil that leaks from downhole machinery and equipment [5]. However, these emulsified oils have complex compositions that include various emulsifiers, such as rosin potassium soap, and acid heavy alkyl benzene sulfonate. When this kind of mine water is discharged to the surface without effective treatment, it quickly mixes with the surface water [6]. Excessive DOM significantly affects the growth of fish and other aquatic life, reducing the health of a body of water [7]. In addition, nitrogen-containing organic matter is a precursor of disinfection by-products (DBPS) in the water-purification process. Trihalomethanes (THMs), haloacetic acids (HAAs), and chloroacetaldehyde are easily generated when ClO_2 is present, and all of these are carcinogens [8]. More importantly, the DOM composition has been found to be an important predictor of CO_2 concentration in streams, linking dissolved CO_2 to DOM quality in streams [9–11]. This could change the river's carbon cycle by modulating CO_2 emissions. Furthermore, DOM has been considered to be the main factor that accounts for CO_2 emissions based on a survey of global reservoirs [12–14]. Therefore, determining the occurrence and migration of DOM in the mine water is not only directly related to the pollution risk of the regional water environment but also has far-reaching significance for the study of the source and transformation of CO_2 .

However, current studies on the DOM of mine water focus on the source and occurrence characteristics of DOM, and there are few reports on the DOM removal rules in the process of mine water treatment. Among them, the most important thing is that the detection of DOM in mine water treatments can be difficult because of its low relative content. Fourier-transform ion cyclotron resonance (FT-ICR), gas chromatography–mass spectrometry (GC–MS), and nuclear magnetic resonance (NMR) spectroscopy provide the structural information of DOM, but they have a relatively low resolution [15]. The excitation emission matrix (EEM) is a three-dimensional fluorescence spectroscopy type of technology that has a sensitive response, high detection accuracy, and does not damage the structure of the sample [16]. It can also be used to perform spectral identification and characterization of fluorescence spectroscopy objects in a multi-component complex system, which is a very

useful spectral fingerprint type of technology [17]. The parallel factor method is a second-order correction method using least squares and can effectively distinguish the interference of repeated peaks in the three-dimensional fluorescence spectrum [18–20]. It eliminates Raman scattering and Rayleigh scattering in the spectrum to achieve the qualitative and quantitative analyses of different components of DOM. This method can provide unique decomposition results and obvious spectral characteristics [21]. In recent years, the method that combined parallel factor analysis (PARAFAC) with the EEM has been widely used to identify DOM in lakes and rivers [22]. Huang et al. used PARAFAC with the EEM to determine DOM levels in a reservoir, and then found that a rainstorm during flooding season significantly increases the land-based DOM in the reservoir, and it is difficult to achieve self-purification [23]. Feng and others analyzed the distribution characteristics and sources of DOM in Taihu Lake using the PARAFAC with the EEM method. It was found that DOM in Taihu Lake was mainly tryptophan-like substances that came from a massive discharge of industrial wastewater and domestic sewage [24]. Although used in lake and river DOM studies, this method is rarely reported in the study of DOM in coal mine water. In addition, the application of the EEM to analyze the change of DOM after mine water treatment has still not been reported.

Here, this paper uses the EEM, combined with the PARAFAC method, to study the compositional characteristics and fluorescence intensity of DOM in the influent and effluent of a mine water treatment station. The goal is to determine the characteristics of DOM in the effluent of mine water and the removal efficiency of different DOM components in the process of mine water treatment. This work provides a scientific basis for the treatment of mine water and for the efficient and green development of the coal industry.

2. Materials and Methods

2.1. Study Area

The Mongolia–Shaanxi border mining area of the Ordos Basin is located in the middle and upper reaches of the Yellow River, which is the most important coal storage and mining area in the country. There are two major coal basins located in Shendong and north Shaanxi. In 2019, the annual coal output exceeded 800 million tons. The border mining area of Inner Mongolia and Shaanxi is located along the border area of Inner Mongolia and Shaanxi. There are other mining areas, such as Shenfu, Yushen, Yuheng, and Hujiet. The climate in this area is arid, with an average annual rainfall of less than 400 mm. Evaporation rates are as high as 1700 mm. The water resources are extremely scarce in the region and are controlled by topography and geological deposits, where the mine water-rich coefficient is generally large. Groundwater leakage during the mining process is severe [25–27].

2.2. Field Sampling

Water samples were collected from 15 large-scale production mine water treatment stations in the Mongolia–Shaanxi border mining area from January to February 2020. Specifically, the Caojatan (109°48′02.61″ E, 38°32′27.12″ N), Mahuangliang (109°56′47″ E, 38°25′31″ N), Yushuwan (109°52′36″ E, 38°28′42″ N), Xiaojihan (109°25′72″ E, 38°22′17.99″ N), Yubujie (109°42′00″ E, 38°24′50″ N), Shilawusu (109°35′00″ E, 38°59′00″ N), Xuemiaotan (109°42′00″ E, 38°25′50″ N), Xiaobaodang (109°45′27″ E, 38°41′50″ N), Bayangaole (109°19′00″ E, 38°42′45″ N), Shuangshan (109°55′01″ E, 38°26′25″ N), Longde (110°03′05″ E, 38°43′58″ N), Jinjie (110°06′00″ E, 38°46′30″ N), Jinjitan (109°42′32″ E, 38°28′15″ N), and Hanglaiwan (109°46′49″ E, 38°24′52″ N) coal mine water treatment plants were selected for this study (Figure 2).

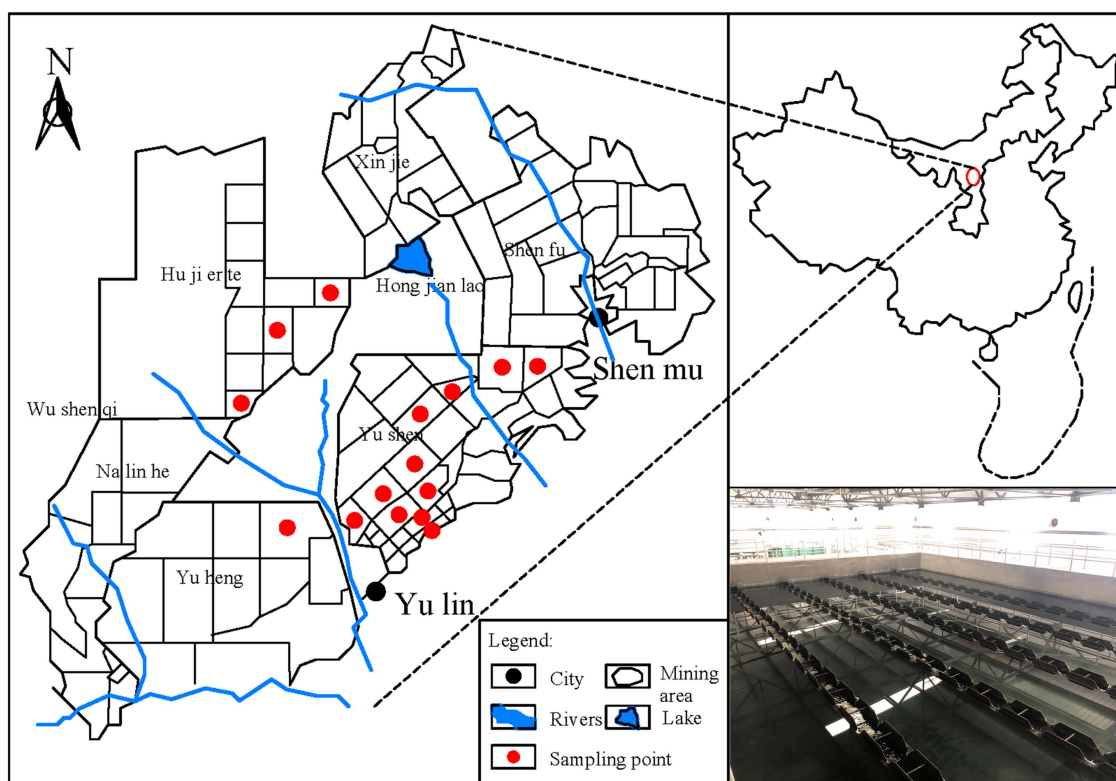


Figure 2. Schematic diagram of sampling points.

Sampling occurred monthly, either in the middle of or late in the month. Volumes of 1 L at the inlet and outlet of the mine water treatment station were sampled each time, and hash SL-1000 was used to measure the pH and temperature on site. Then, it was stored in a brown glass bottle and sent to the Institute of Nuclear Energy and New Energy Technology, Tsinghua University for testing within 24 h. Multi-point sampling of the same coal mine water was conducted to eliminate abnormalities, and the average value was used for analysis.

Additionally, the Caojiatan coal mine water treatment station was used throughout the paper as a typical example. The treatment station uses the “grading treatment” technical route, as shown in Figure 3. The mine water first passes through the coagulant PAC (polyaluminum chloride), which is added to the pre-mixing tank to increase the size of suspended particles in the body of water. After it is fully mixed, it is discharged to the dosing workshop by a lifting pump, and PAMs (polyacrylamides) are added. Then, water flows into transmission tank 1. This part of the water is usually used for coal washing, which has lower water-quality requirements. Additionally, excess water enters the valveless filter to complete the filtration unit operation, which is about 520 m³/h. At random, mine water enters transmission tank 2 to be filtered. The remaining water resources of about 240 m³/h are finally sent to the ultrafiltration unit through the lifting pump for processing.

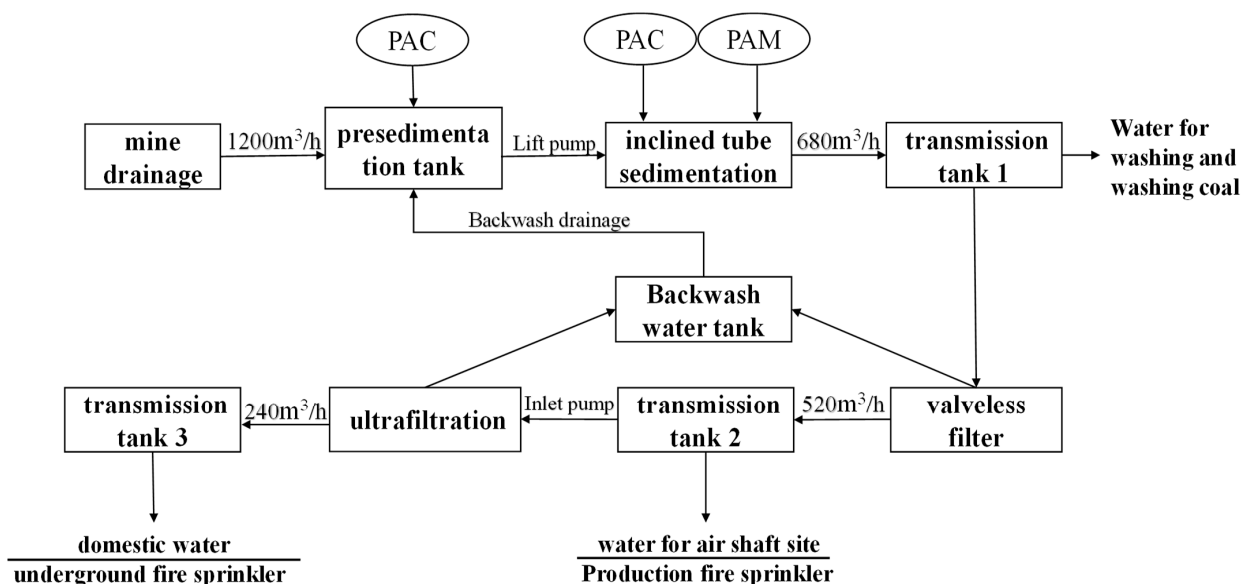


Figure 3. Process flowchart of mine water treatment in the Caojiatan coal mine.

2.3. Parameters Measuring

2.3.1. Physicochemical Properties

With reference to the Chinese Groundwater Quality Standard (GB14848-2017), 20 water-quality parameters of different coal mine effluents in the study area were analyzed [28]. Water-quality parameters were measured according to the U.S. Environmental Protection Agency (USEPA) digestion colorimetry of the HACH® standard method, HJT399-2007, and HJ536-2009 (Table 1).

Table 1. Analysis index and methods.

Project	Analytical Method
pH	Glass electrode method
COD	Potassium permanganate method
copper	Atomic absorption spectrophotometry
Fluoride	Ion chromatography
Sulfate	Flame atomic absorption spectrophotometry
chloride	Ion chromatography
NO ₃ ⁻	UV spectrophotometry
Mn	Flame atomic absorption spectrophotometry
TDS	105 °C dry weight method
Ec	Glass electrode method
NO ₂ ⁻	Spectrophotometry
NH ₄ ⁺	Spectrophotometry
TOC	Combustion oxidation—non-dispersive infrared absorption method
UV ₂₅₄	spectrophotometric method
EEMs	Three-dimensional fluorescence spectrometric

2.3.2. TOC/UV254

A TOC-VCPH analyzer (Shimadzu, Japan) was used to determine the TOC (total organic carbon) content of mine water using the combustion oxidation non-dispersive infrared absorption method. The UV₂₅₄ was measured with an ultraviolet-visible spectrophotometer (UV-1800, Shimadzu, Japan).

2.3.3. EEM

The EEM has the advantages of high sensitivity and strong operability. It was recently used in the determination of DOM in various bodies of water. In this study, a fluorescence spectrophotometer (Hitachi F-7000, Tokyo, Japan) was used to analyze the DOM components. The tests were performed at room temperature. A 1 cm quartz cuvette with light transmission on all sides was used. The emission wavelength range was set to 280–550 nm with an interval of 5 nm. The excitation wavelength range was 220 to 480 nm with an interval of 2 nm, and the width of the excitation and emission slits were both 5 nm. During the tests, the sensitivity of the instrument was set to high sensitivity, and the scanning speed was set to 2000 nm/min to remove the background noise. Each time, the sample was tested with ultrapure water as a blank under the same test conditions.

The humification index (HIX) is defined as the ratio of the integrated fluorescence intensity in the wavelength band of 435–480 nm and 300–345 nm when the excitation wavelength is 255 nm. A larger index indicates a higher degree of DOM [29]. The freshness index (BIX) is defined as the emission wavelength of 380 nm and 430 nm when the excitation wavelength is 310 nm.

2.4. Statistical Analysis

The traditional EEM cannot be used to determine various compounds with different concentrations within a sample because of the inner-filter effect, resulting in some organic compounds that cannot be detected and resulting in large errors in the results. Using the PARAFAC method to process EEM data can help to accurately analyze the component types of DOM and to distinguish the various peaks in a sample with multiple organic compounds. The alternating-least-squares method was used to decompose the three-dimensional dataset $I \times J \times K$ of EEMs into three matrices, namely A (score matrix), B, and C (load matrix), respectively, and elements a_{if} , b_{jf} , and c_{kf} , respectively. The equations are as follows:

$$X_{jik} = \sum_{f=1}^F a_{if} b_{jf} c_{kf} + e_{jik};$$

$$i = 1, 2, \dots, I;$$

$$j = 1, 2, \dots, J;$$

$$k = 1, 2, \dots, K$$
(1)

where f represents a certain fluorescent component, and F is the total number of fluorescent components.

In this study, the PARAFAC algorithm was implemented by the DOM Flour toolbox in MATLAB (R2014 a), substituting into the N-way module [30]. The data array had 26 emission wavelengths and 41 excitation wavelengths. The spectrum of pure water was first subtracted from the EEM sample spectrum. The data were then imported into MATLAB for further refinement using the DOM Flour toolbox. To eliminate Raman scattering and Rayleigh scattering, the two-multiplication method combined the confidence, residual, square error, and other parameters in PARAFAC to finally obtain the optimal composition and fluorescence intensity [31]. This procedure was conducted for each sample, generating a 26×41 matrix for each sample. Contour maps were then drawn to showcase the data [32].

3. Results

3.1. Comparison of Biogeochemical Characteristics

The excitation spectrum wavelengths compared to the emission spectrum were plotted for the 15 samples (Figure 4).

It was found that the DOM-absorption peak intensity of mine water in three coal mines was relatively high. The Caojatan and Xiaobaodang coal mines showed partial pollution characteristics in zone 3, and the Longde coal mine in zone 5. This zone represents tryptophan components in the protein-like components, which is mostly produced by the point source discharge of industrial wastewater [33,34]. Moreover, DOM in the mining area was

divided into zones II (Ex: 200 nm–250 nm, Em: 330 nm–370 nm), III (Ex: 200 nm–250 nm, Em: 370 nm–450 nm), and V (Ex: 250–300, Em: 330–370)

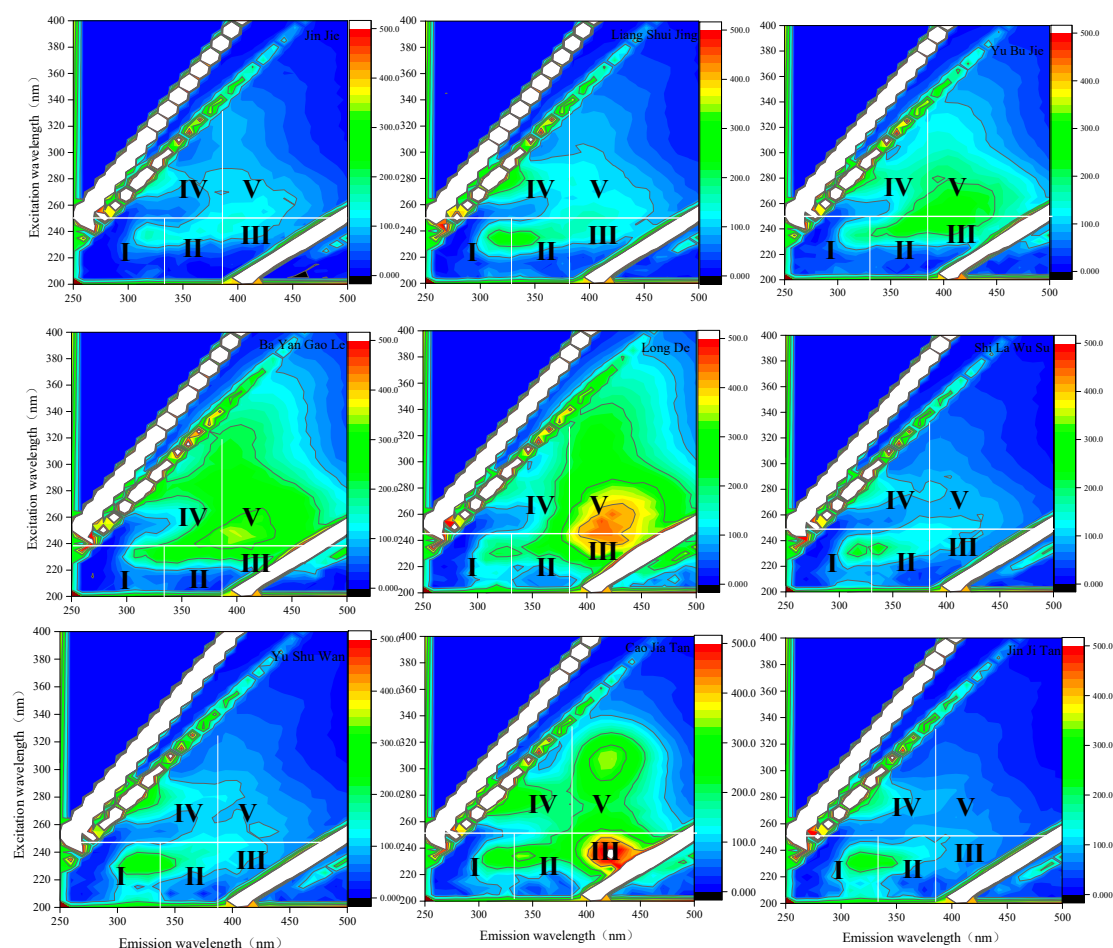


Figure 4. DOM distribution of the water samples from 15 coal mine water treatment stations.

To determine the occurrence characteristics of organic pollutants in mine water in the mining area and to quantitatively evaluate the characteristics of DOM components, the EEM data of the mine water treatment station were processed using the parallel factor method (Figure 5).

Four components were identified in the effluent samples of all the mine water treatment stations by the parallel factor method (Figure 5). C1 (Ex/Em: 260 nm/410 nm) was identified as a fulvic-acid-like substance in the ultraviolet region [35,36]. C2 (Ex/Em: 230/330) was identified as a protein tryptophan-like substance [37,38]. C3 (Ex/Em: 240/370 and 230/310) was identified as a fulvic-acid-like substance in the ultraviolet region [39]. C4 (Ex/Em: 220/310) was identified as a protein tyrosine-like substance [39,40]. The fulvic acids in the C1 and C3 ultraviolet regions generally exist in sandy soil [41]. It is transferred to groundwater through rainfall and other processes. Because of the aromatic ring structure of humic acid, the chemical bond is not broken in the conventional treatment stage. Therefore, there is still a high proportion of it in the effluent. The C2 component is derived from a tryptophan-like acid. In addition to numerous microbial activities, it mainly comes from the by-products of polycyclic aromatic hydrocarbons or their derivatives during processing [42]. C4, which is classified as the protein lysine, mostly comes from point source pollution formed by large-scale human activities [43]. Because mine water exists in the subsurface over geologic time periods (i.e., thousands to hundreds of millions of years) and has no plant photosynthesis, the tryptophan and tyrosine components are mainly caused by the leakage of underground petroleum pollutants [44].

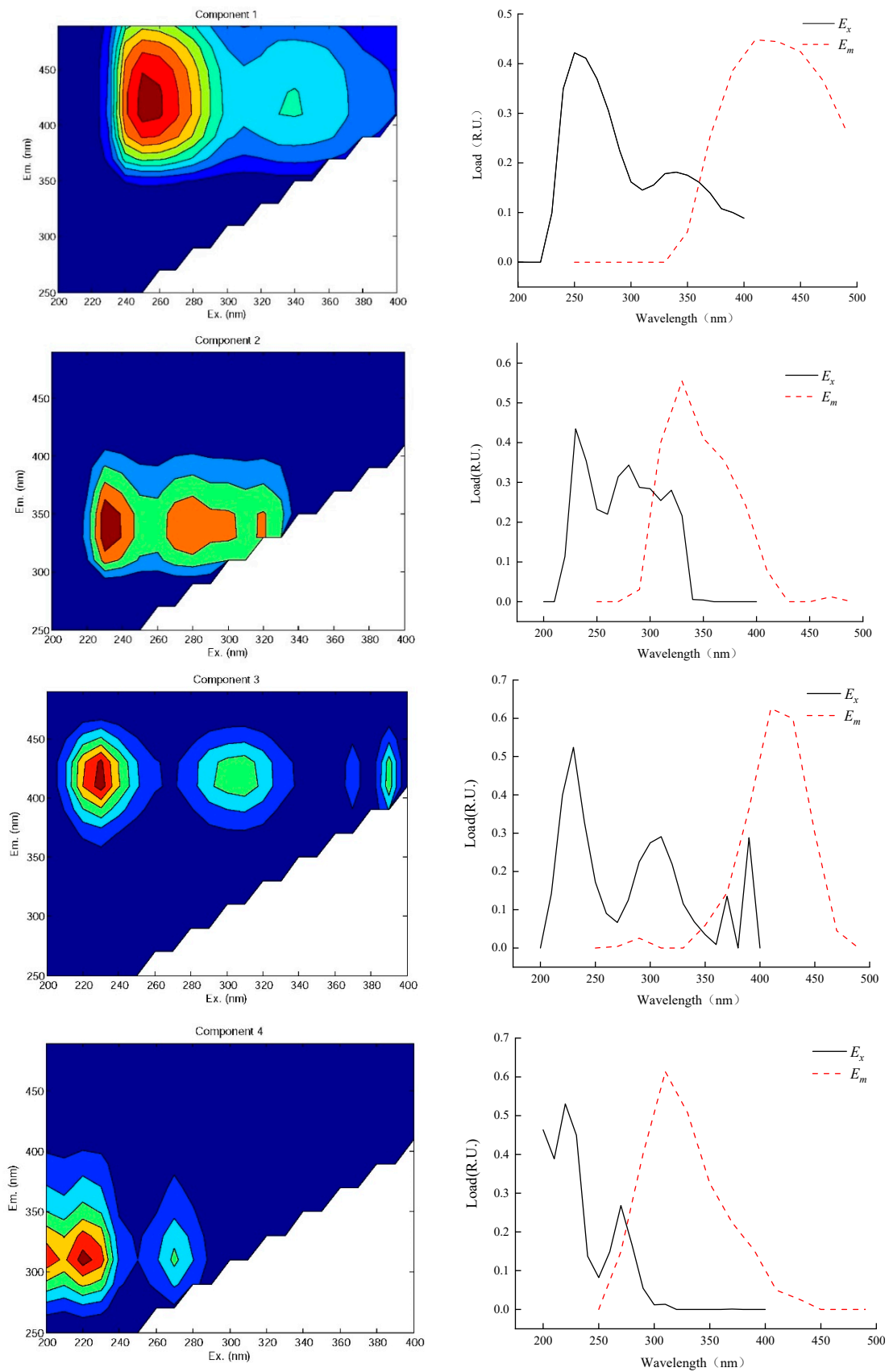


Figure 5. Schematic diagram of mine water effluent composition based on parallel factor.

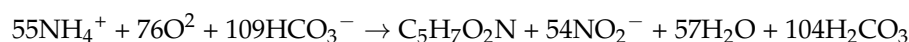
3.2. Water Quality and DOM Characteristics of the Influent and Effluent Water in the Caojiatan Coal Mine Water Treatment Station

After water is passed through the mine water treatment stations, different pollution components show the change characteristics of travel alienation. To further evaluate the removal effectiveness of different pollution components by the mine water treatment process, the rates of removal of the components were classified into four classes as follows: Class A: large removal (removal efficiency > 70%), indicating that the removal effect of this type of pollution component is good; Class B: slightly reduced (20% < removal efficiency < 70%), indicating that the pollutant can be removed; Class C: essentially unchanged (removal efficiency < 20%), indicating that there is no obvious removal effect on the pollution components; Class D: the concentration increased (removal efficiency is negative), indicating that a pollution component is introduced during the treatment process (Table 2).

Table 2. Classification of treatment capacity of different pollution factors in the Caojiatan mine water treatment station.

Grade	Pollutant	Removal Rate
A	COD	94.3%
	NO ₂ [−]	90%
	BIX	51.12%
	Cu ²⁺	50%
B	HIX	45.82%
	TOC	47.79%
	F [−]	24.11%
	FI	13.37%
	Ec	1.64%
	TDS	2.5%
C	NH ₄ ⁺	0%
	Mn	0%
	NO ₃ [−]	−85.47%
D	UV ₂₅₄	−300%

The results show that the treatment process has a good effect on the removal of COD and NO₂[−] in the discharged mine water with removal efficiencies that are greater than 90%. This is because the contribution of suspended solids to COD can reach 90%. This process is highly effective at removing suspended solids in the discharged water. The removal of NO₂[−] is mainly due to its reducibility. Under the aerobic conditions of the existing nitrifying bacteria, NO₂[−] reacts with an oxidant in the water to form NO₃[−]. It is speculated that hypochlorite, with strong oxidation, may be added to the disinfection link [45]. This is also the reason that NO₃[−] increases in concentration during the treatment process. The reaction is essentially comprised of “one-step nitrification” and “two-step nitrification”.



It was found that there was no change in NH₄⁺ after treatment, indicating that only the second-stage nitrification reaction occurred and that NO₂[−] is transformed into NO₃[−]. This is due to a lack of nitrifying bacteria, which are required for one-step nitrification in the system. In addition, the removal efficiencies of TOC, Hix, and Bix in the water used in the treatment system were about 50%, indicating that the whole system has the ability for organic matter removal, although some organic matter cannot be removed after treatment. The system has a certain removal capacity for Cu²⁺ and F[−] because Cu²⁺ can form complex ions with the coagulant in the coagulation process. Under the action of van der Waals forces, Cu²⁺ and F[−] are adsorbed on the flocs, which then settle and are removed from the tank [46]. However, the system showed a poor treatment capacity for several types of organic compounds and had little removal effect on EC, TDS, NH₄⁺, and Mn. This is

because this process cannot effectively remove most of the dissolved solids in the mine water, and so the membrane method needs to be used for removal [47].

The concentrations of NO_3^- and UV_{254} increased significantly after treatment. In water, this mostly represented aromatic hydrocarbons and heterocyclic organic compounds with a benzene ring structure and is consistent with the research results in the literature [48,49] (Figure 6).

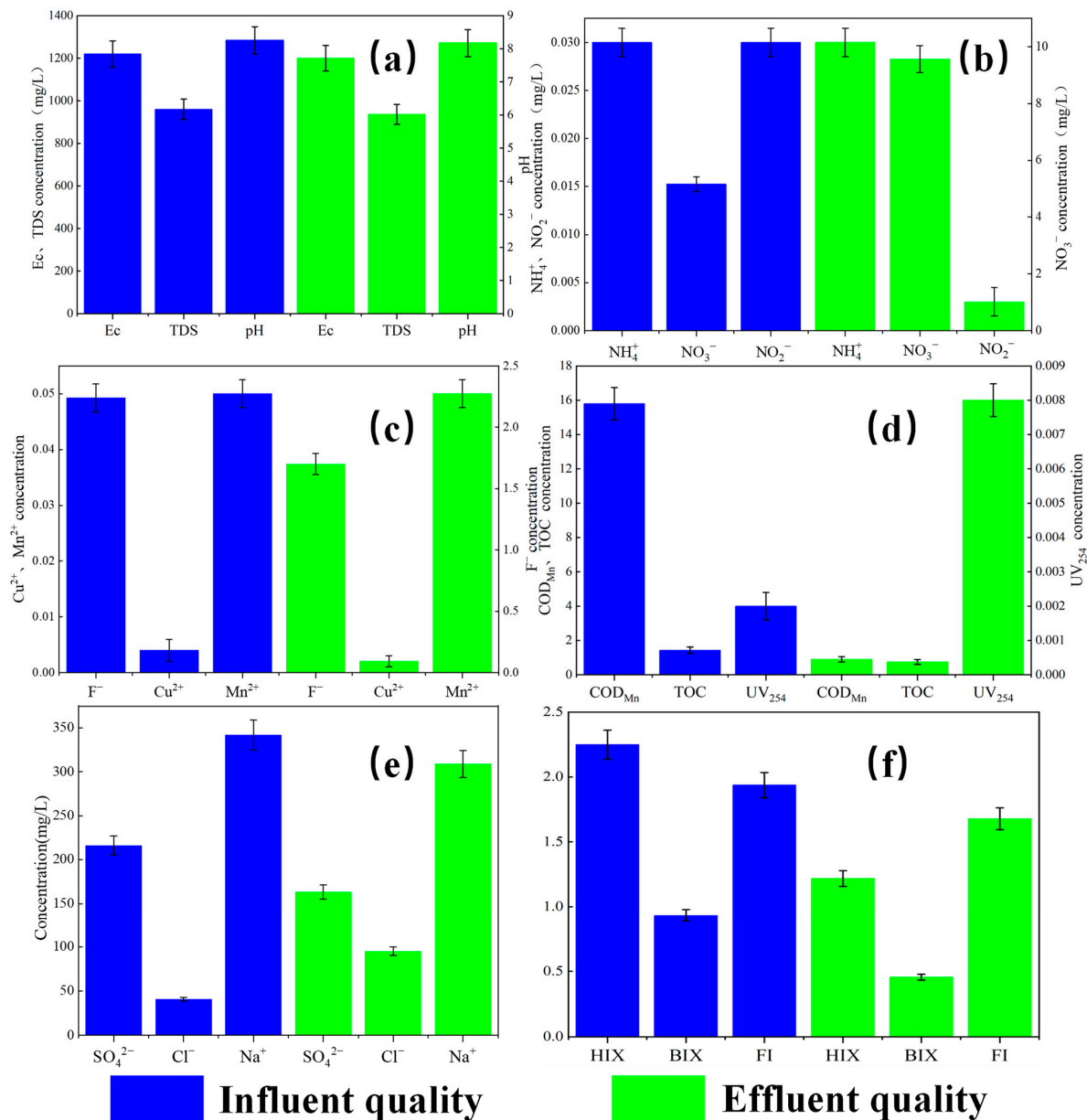


Figure 6. Characteristics of influent and effluent water quality at the Caojiatan mine water treatment station. (a,c,e) are inorganic components of the mine water; (b,d,f) are the organic components.

3.3. DOM Characteristics of the Water Influent and Effluent of Caojiatan Mine Water Treatment Station

After treatment, the protein-like components decreased from 67.59% to 40.18%, indicating that the process can remove some of the petroleum pollutants found in mine water. To further explore the removal effectiveness of different DOM components in the treatment process, the EEM of the influent and effluent from the mine water treatment station were compared and studied. Three DOM components were identified in the influent, including the ultraviolet humus tryptophan-like component and the tyrosine-like component

(Figure 7). In the effluent of the mine water treatment station, two DOM components were identified, namely the fulvic-acid-like component and the protein tyrosine-like component (Figure 8). The fluorescence intensity of the fulvic-acid-like component increased from 334.7272 a.u to 440.3296 a.u after treatment, and the fluorescence intensity of the protein tyrosine-like component decreased from 330.1814 a.u to 295.7762 a.u after treatment.

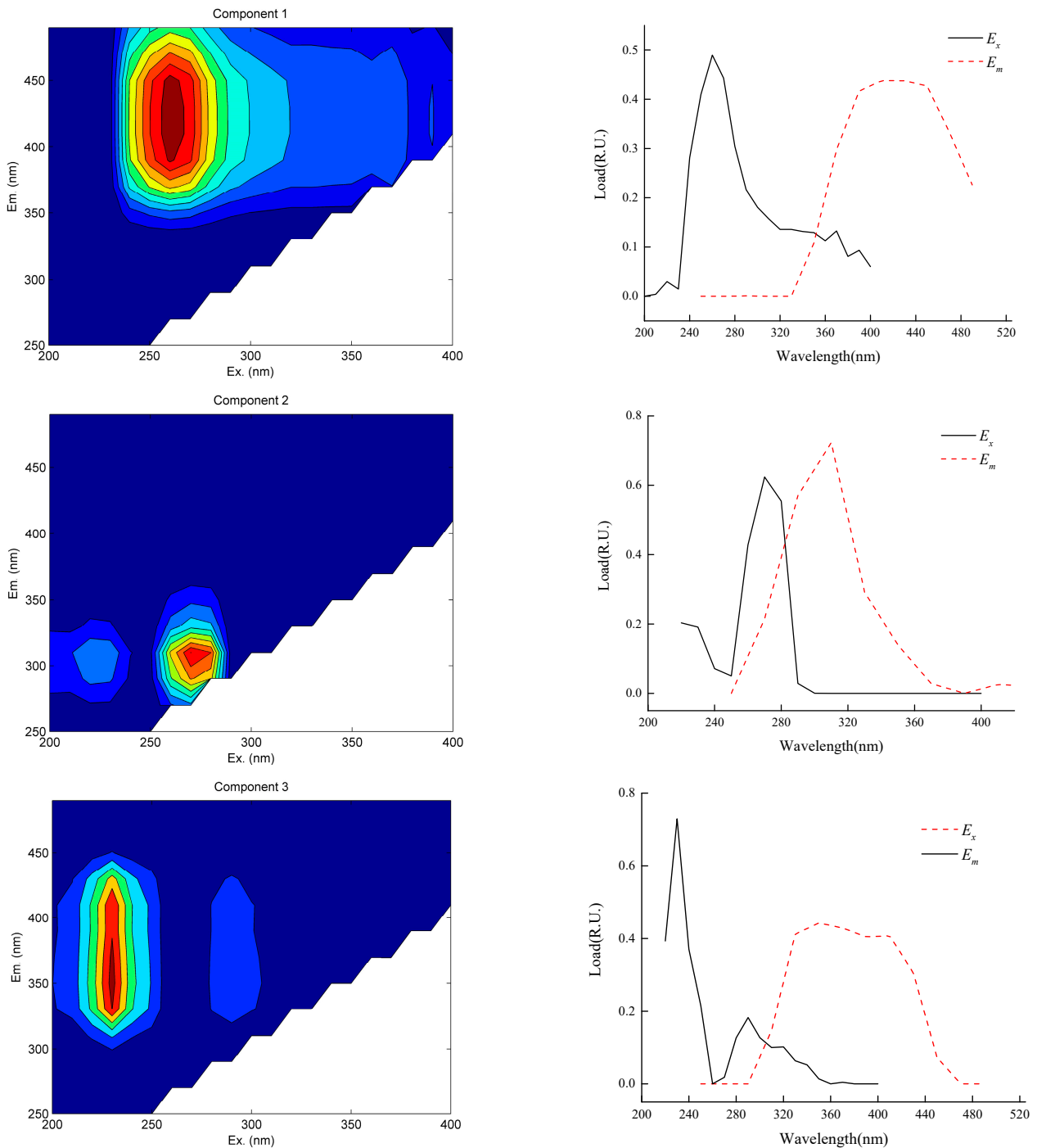


Figure 7. DOM characteristics of influent at the Caojiatan mine water treatment station.

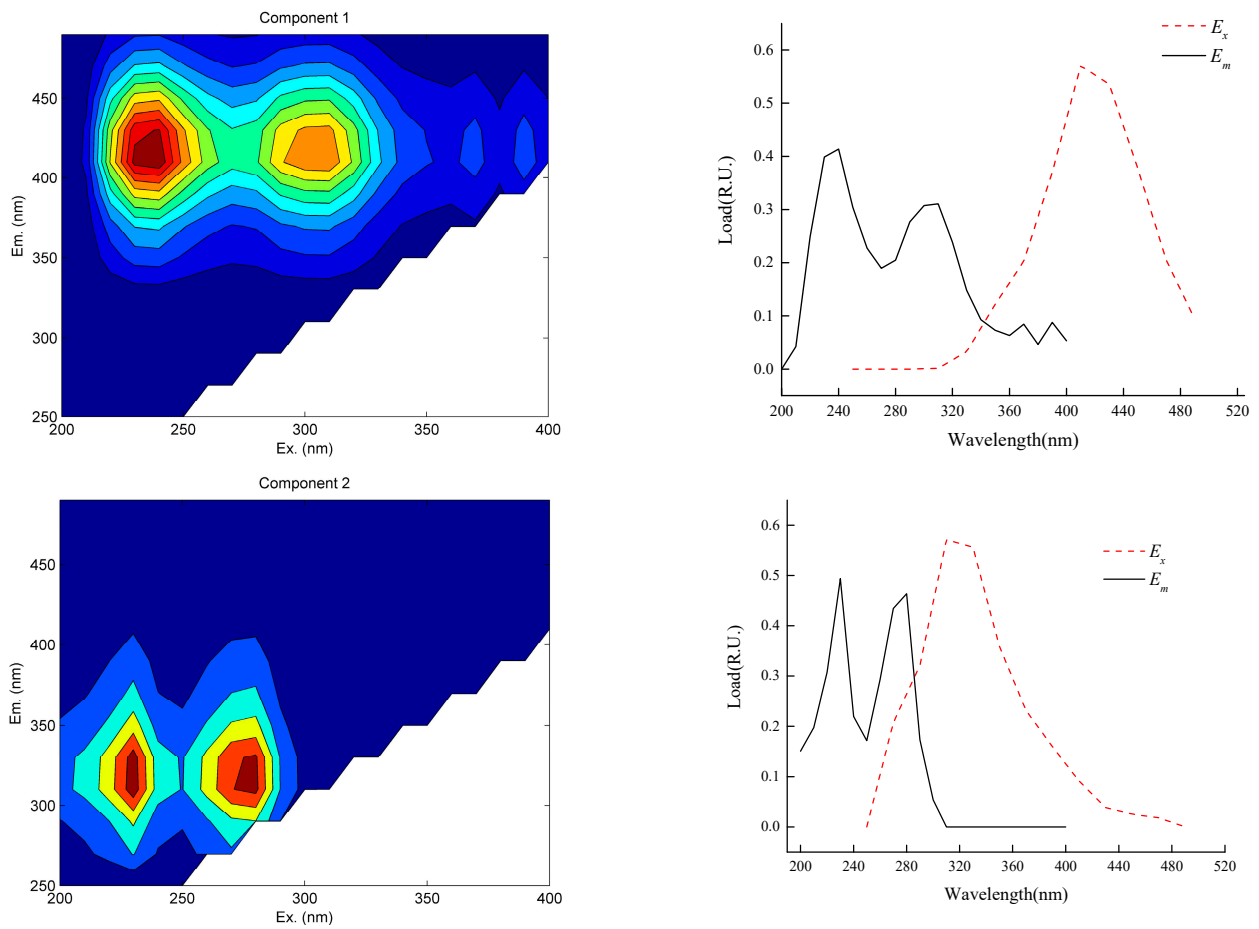


Figure 8. DOM characteristics of effluent at the Caojiatan mine water treatment station.

This is because the protein tyrosine-like fluorescence is composed of several simple molecular structures, such as amino proteases and peptides, with fluorescent groups. Tryptophan is used to represent fatty hydrocarbons and alkanes with relatively simple molecular structures, and so it easily degrades [49–51] under the coagulation–filtration–disinfection treatment (Figure 9).

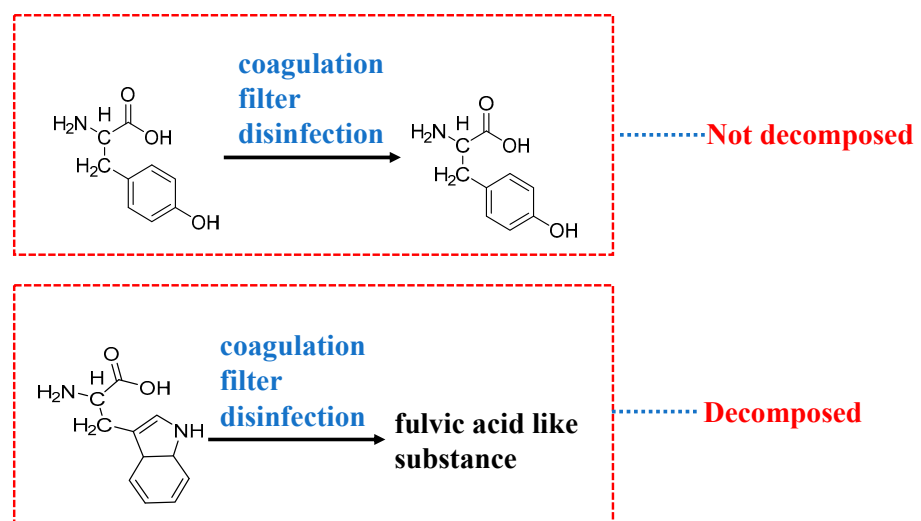


Figure 9. Schematic diagram of DOM removal in mine water.

DOM can somewhat promote the coagulation process. Alkane DOM is removed from water by being adsorbed on the floc surface during the coagulation process [52–54]. By contrast, it should be noted that the protein-like tryptophan component was completely removed when the influent was treated. This is because tyrosine in protein-like components is often used to represent aromatic hydrocarbons, such as phenols, dichlorobenzene, and benzene, with complex structures in petroleum pollutants [55–57]. However, the whole treatment system has a lack of advanced oxidation units, and the aromatic components in petroleum pollutants have strong molecular bonds and fail to completely fracture the benzene ring [58]. Although phenol can have two types of reactions, where either the C-O bond or O-H bond break, it is difficult to break the C-O bond because of the p- π conjugation effect.

The fluorescence intensity of the fulvic-acid-like compounds increased from 334.7272 a.U to 440.3296 a.U, which is consistent with results reported in the literature [59]. The increase in the fluorescence intensity of the fulvic-acid-like components may be due to the transformation of a few classified protein components of fulvic-acid-like components during the treatment process. Furthermore, chlorine (chloramine) disinfectant increased the concentration of the AOC (assimilable organic carbon) in the effluent [60–62].

In addition, it is difficult to dissolve petroleum substances leaked by an underground shearer in water due to their small polarity. When an emulsifier with a polar micelle hydraulic support is added to the influent, the solute molecules are wrapped and positioned in a lipophilic core of the micelle because the solute molecules have an affinity for the nonpolar tail of the normal-phase micelle. A stable boundary film is formed on the oil–water interface. Conventional physical methods cannot break the boundary membrane between oil and water, resulting in the continuous accumulation of oil molecules throughout the life-cycle of the mine water. Therefore, to achieve the efficient removal of petroleum pollutants, an oxidation unit must be introduced into the system to break the hydrocarbon carbon rings.

3.4. Discussion on Removal Technology of Petroleum Pollutants Based on Tyrosine Components

It has been found that the coagulation–sedimentation process has a removal efficiency of only 14% for oil pollutants in mine water (Table 3), whereas the removal efficiency can reach 62% by means of electrolytic air flotation with a sand filter [63]. The oil-removal processes of ten coal mines in China were further obtained (Table 3) through a search of the literature. When adsorbents, such as activated carbon, were added, the removal efficiency of oil pollutants reached more than 80% [64], but this approach has some problems regarding high costs and difficult regeneration. In terms of absolute content, only the method of ozone oxidation in investigated samples can minimize the concentration of petroleum pollutants in water (0.19 mg/L) [65]. For the removal of oil pollutants in water, coagulation filtration and other methods can reduce 500–1000 mg/L oil in raw water down to 20 mg/L [66]. Oil pollutants can be reduced to 5 mg/L using Fenton reagent oxidation alone.

Table 3. Trace oil pollutants in mine water.

Mining Area	Before Treatment (mg/L)	Treatment Process	After Treatment (mg/L)	Removal Rate (%)
Yanzhou	6	Coagulation sedimentation + oil scraper	0.6	90%
Changzhi	0.8	Ozone oxidation + activated carbon adsorption	0.019	97%
Huainan	3.388	Coagulation + filtration + adsorption	0.136	96%
Huainan	3.85	Coagulation + sedimentation	3.3	14%
Datong	0.29	Electrolytic air flotation + sand filter	0.11	62%
Datong	0.72	Add C-F-O adsorbent	0.05	93%
HuaiBei	4.2	TiO ₂ supported activated carbon adsorption	0.84	80%
Fushun	17.3	Lime softening and degreasing	4.3	75%

The key to the removal of emulsified oil in mine water is to break the “protective” boundary membrane of tyrosine components, which is called “demulsification”. Currently, commonly used demulsification methods include ozone oxidation, flocculation, and Fenton reagent oxidation. Most methods have significant removal effects on high-concentration oil pollution but poor removal effects on trace oil pollutants in mine water. O^3 has an obvious removal effect on amino acids in water, and the removal efficiency of most amino acids can reach more than 65% [67]. The oil-removal unit is constructed separately, where high molecular organic matter is degraded into small molecular compounds by ozone oxidation. The smaller particles are flocculated and settled by adding agents, such as PAC and PAM. Finally, the flocs and suspended solids with large particle sizes in the wastewater are caused to float on top of the unit using the dissolved-air-flotation method. After their removal, the effluent meets the discharge standards.

4. Conclusions

1. The effluent from the mine water treatment station mainly contains four components. There is fulvic-acid-like acid in the C1/C3 ultraviolet region; the fulvic-acid-like acid generally exists in sandy soil and moves to the groundwater through rainfall and other processes. The C2 component is derived from tryptophan-like acids. In addition to the emulsified oil produced by a large number of microbial activities and underground shearer leakage, the C4 component is mainly derived from point source pollution formed by large-scale human activities.
2. The treatment effect of the coagulation–filtration–disinfection process on COD and nitrite can reach more than 90% removal. The removal efficiency of TOC can reach 50%. After treatment, some of the TOC that cannot be removed remains. At the same time, the system has a poor treatment capacity for several organic ions, including EC, TDS, NH_4^+ , SO_4^{2-} , Cl^- , and Mn, and has a certain removal capacity for Cu^{2+} and F^- .
3. Through the coagulation–filtration–disinfection process, protein-like tryptophan substances in the water are completely removed. The fluorescence intensity of the fulvic-acid-like components increases from 334.7272 a.U to 440.3296 a.U, whereas the fluorescence intensity of the protein tyrosine-like components decreases from 330.1814 a.U to 295.7762 a.U. This is because the alkanes, cycloalkanes, and other fatty hydrocarbons of the oil pollutants in the mine water are removed during the treatment process. On the basis of this, an ozone air-flotation combination-removal process is proposed to be suitable for the removal of emulsified oil in mine water.

Author Contributions: X.Z.: Conceptualization, Investigation, Writing—original draft. S.D.: Writing—reviewing and editing. P.J.: Visualization, Writing—reviewing and editing. J.L.: Supervision, Project administration. J.Y.: Methodology. Y.H.: Investigation, Project administration. All authors have read and agreed to the published version of the manuscript.

Funding: This research was funded by [Natural Science Foundation of Shaanxi Province, China] grant number [2021]Q-948].

Data Availability Statement: The data presented in this study are available on request from the corresponding author. The data are not publicly available due to [Privacy involving relevant coal mining enterprises].

Acknowledgments: All individuals included have consented to the acknowledgement.

Conflicts of Interest: The authors declare no conflict of interest.

References

1. Fuß, T.; Behounek, B.; Ulseth, A.J.; Singer, G.A. Land use controls stream ecosystem metabolism by shifting dissolved organic matter and nutrient regimes. *Freshw. Biol.* **2017**, *62*, 582–599. [[CrossRef](#)]
2. Monteith, D.T.; Stoddard, J.L.; Evans, C.D.; de Wit, H.A.; Forsius, M.; Høgåsen, T.; Wilander, A.; Skjelkvåle, B.L.; Jeffries, D.S.; Vuorenmaa, J.; et al. Dissolved organic carbon trends resulting from changes in atmospheric deposition chemistry. *Nature* **2007**, *450*, 537–540. [[CrossRef](#)] [[PubMed](#)]

3. Parr, T.B.; Cronan, C.S.; Ohno, T.; Findlay, S.E.G.; Smith, S.M.C.; Simon, K.S. Urbanization changes the composition and bioavailability of dissolved organic matter in headwater streams. *Limnol. Oceanogr.* **2015**, *60*, 885–900. [[CrossRef](#)]
4. Zhang, X.; Yang, J.; Wang, H. Study on characteristics and sources of DOM in mine water in the middle of the Yellow River Basin Based on parallel factor method. *J. China Coal Soc.* **2021**, 1–14. [[CrossRef](#)]
5. Zou, Y.; Lv, R.; Yang, J. Three-dimensional excitation emission matrix fluorescence spectroscopic characterization of dissolved organic matter in coal mine water. *J. China Coal Soc.* **2012**, *37*, 1396–1400.
6. Weber, J.H.; Wilson, S.A. The isolation and characterization of fulvic acid and humic acid from river water. *Water Res.* **1975**, *9*, 1079–1084. [[CrossRef](#)]
7. Demars, B.O.L.; Friberg, N.; Thornton, B. Pulse of dissolved organic matter alters reciprocal carbon subsidies between autotrophs and bacteria in stream food webs. *Ecol. Monogr.* **2020**, *90*, e01399. [[CrossRef](#)]
8. Awad, J.; Fisk, C.A.; Cox, J.W.; Anderson, S.J.; van Leeuwen, J. Modelling of THM formation potential and DOM removal based on drinking water catchment characteristics. *Sci. Total Environ.* **2018**, *635*, 761–768. [[CrossRef](#)]
9. Bodmer, P. Linking Carbon Dynamics in Stream Ecosystems to Dissolved Organic Matter Quality. Ph.D. Dissertation, Freie Universität Berlin, Berlin, Germany, 2016.
10. Bodmer, P.; Heinz, M.; Pusch, M.; Singer, G.; Premke, K. Carbon dynamics and their link to dissolved organic matter quality across contrasting stream ecosystems. *Sci. Total Environ.* **2016**, *553*, 574–586. [[CrossRef](#)]
11. Glatzel, S.; Kalbitz, K.; Dalva, M.; Moore, T. Dissolved organic matter properties and their relationship to carbon dioxide efflux from restored peat bogs. *Geoderma* **2003**, *113*, 397–411. [[CrossRef](#)]
12. Barros, N.; Cole, J.J.; Tranvik, L.J.; Prairie, Y.T.; Bastviken, D.; Huszar, V.L.M.; del Giorgio, P.; Roland, F. Carbon emission from hydroelectric reservoirs linked to reservoir age and latitude. *Nat. Geosci.* **2011**, *4*, 593–596. [[CrossRef](#)]
13. Duan, H.; Feng, L.; Ma, R.; Zhang, Y.; Loiselle, S.A. Variability of particulate organic carbon in inland waters observed from MODIS Aqua imagery. *Environ. Res. Lett.* **2014**, *9*, 084011. [[CrossRef](#)]
14. Prairie, Y.T.; Alm, J.; Beaulieu, J.; Barros, N.; Battin, T.; Cole, J.; del Giorgio, P.; DelSontro, T.; Guérin, F.; Harby, A.; et al. Greenhouse Gas Emissions from Freshwater Reservoirs: What Does the Atmosphere See? *Ecosystems* **2018**, *21*, 1058–1071. [[CrossRef](#)] [[PubMed](#)]
15. Hertkorn, N.; Harir, M.; Koch, B.P. High field NMR Spectroscopy and FTICR Mass Spectrometry: Powerful Discovery Tools for the Characterization of Marine Dissolved Organic Matter. In Proceedings of the EGU General Assembly Conference Abstracts, Vienna, Austria, 22–27 April 2012; p. 12595.
16. Mosher, J.J.; Kaplan, L.A.; Podgorski, D.C.; McKenna, A.M.; Marshall, A.G. Longitudinal shifts in dissolved organic matter chemogeography and chemodiversity within headwater streams: A river continuum reprise. *Biogeochemistry* **2015**, *124*, 371–385. [[CrossRef](#)]
17. Zhou, Z.; Liu, Z.; Guo, L. Chemical evolution of Macondo crude oil during laboratory degradation as characterized by fluorescence EEMs and hydrocarbon composition. *Mar. Pollut. Bull.* **2013**, *66*, 164–175. [[CrossRef](#)] [[PubMed](#)]
18. Bianchi, T.S.; Osburn, C.; Shields, M.R.; Yvon Lewis, S.; Young, J.; Guo, L.; Zhou, Z. Deepwater Horizon Oil in Gulf of Mexico Waters after 2 Years: Transformation into the Dissolved Organic Matter Pool. *Environ. Sci. Technol.* **2014**, *48*, 9288–9297. [[CrossRef](#)]
19. He, D.; Wang, K.; Pang, Y.; He, C.; Li, P.; Li, Y.; Xiao, S.; Shi, Q.; Sun, Y. Hydrological management constraints on the chemistry of dissolved organic matter in the Three Gorges Reservoir. *Water Res.* **2020**, *187*, 116413. [[CrossRef](#)]
20. Wen, Z.; Song, K.; Shang, Y.; Zhao, Y.; Fang, C.; Lyu, L. Differences in the distribution and optical properties of DOM between fresh and saline lakes in a semi-arid area of Northern China. *Aquat. Sci.* **2018**, *80*, 1–12. [[CrossRef](#)]
21. Lyu, L.; Liu, G.; Shang, Y.; Wen, Z.; Hou, J.; Song, K. Characterization of dissolved organic matter (DOM) in an urbanized watershed using spectroscopic analysis. *Chemosphere* **2021**, *277*, 130210. [[CrossRef](#)] [[PubMed](#)]
22. Li, W.T.; Chen, S.Y.; Xu, Z.X.; Li, Y.; Shuang, C.D.; Li, A.M. Characterization of Dissolved Organic Matter in Municipal Wastewater Using Fluorescence PARAFAC Analysis and Chromatography Multi-Excitation/Emission Scan: A Comparative Study. *Environ. Sci. Technol.* **2014**, *48*, 2603–2609. [[CrossRef](#)] [[PubMed](#)]
23. Li, C.Y.; Huang, T.L.; Wen, C.C.; Liang, W.G.; Lin, Z.S.; Yang, S.Y.; Li, K.; Cai, X.C. Influence of Storm Runoff on the Spectral Characteristics of Dissolved Organic Matter (DOM) in a Drinking Water Reservoir During the Flood Season. *Huanjing kexue* **2021**, *42*, 1391–1402. [[CrossRef](#)]
24. Feng, W.; Zhu, Y.; Wu, F. The fluorescent characteristics and sources of dissolved organic matter in water of Tai Lake. *Acta Sci Circumst* **2016**, *36*, 475–482. [[CrossRef](#)]
25. Khan, S.; Shahnaz, M.; Jehan, N.; Rehman, S.; Shah, M.T.; Din, I. Drinking water quality and human health risk in Charsadda district, Pakistan. *J. Clean. Prod.* **2013**, *60*, 93–101. [[CrossRef](#)]
26. Li, Z.; Peng, H.; Xie, B.; Liu, C.; Nie, X.; Wang, D.; Huang, M.; Xiao, H.; Shi, L.; Zhang, X.; et al. Dissolved organic matter in surface runoff in the Loess Plateau of China: The role of rainfall events and land-use. *Hydrol. Process.* **2020**, *34*, 1446–1459. [[CrossRef](#)]
27. Yang, J.; Wang, Q.; Wang, T.; Zhang, X. Variation characteristics of mine water quality during maintenance of underground fully mechanized mi-ning equipment in Shenfu mining area. *J. China Coal Soc.* **2019**, *44*, 3710–3718. [[CrossRef](#)]
28. Fu, Y.; He, K.; Zhou, C.; Mao, Y. Improvement of Saline-Alkaline Soil via Flue Gas Desulfurization Gypsum and Safety Analysis of the Associated Heavy Metals. *J. Phys. Conf. Ser.* **2021**, *1838*, 012051. [[CrossRef](#)]
29. Zhou, Y.; Davidson, T.A.; Yao, X.; Zhang, Y.; Jeppesen, E.; de Souza, J.G.; Wu, H.; Shi, K.; Qin, B. How autochthonous dissolved organic matter responds to eutrophication and climate warming: Evidence from a cross-continental data analysis and experiments. *Earth Sci. Rev.* **2018**, *185*, 928–937. [[CrossRef](#)]

30. Andersson, C.A.; Bro, R. The N-way Toolbox for MATLAB. *Chemom. Intell. Lab. Syst.* **2000**, *52*, 1–4. [[CrossRef](#)]
31. Bahram, M.; Bro, R.; Stedmon, C.; Afkhami, A. Handling of Rayleigh and Raman scatter for PARAFAC modeling of fluorescence data using interpolation. *J. Chemom.* **2006**, *20*, 99–105. [[CrossRef](#)]
32. Zhang, K.; Gao, J.; Men, D.; Zhao, X.; Wu, S. Insight into the heavy metal binding properties of dissolved organic matter in mine water affected by water-rock interaction of coal seam goaf. *Chemosphere* **2021**, *265*, 129134. [[CrossRef](#)]
33. Del Castillo, C.E.; Coble, P.G.; Conmy, R.N.; Müller Karger, F.E.; Vanderbloemen, L.; Vargo, G.A. Multispectral in situ measurements of organic matter and chlorophyll fluorescence in seawater: Documenting the intrusion of the Mississippi River plume in the West Florida Shelf. *Limnol. Oceanogr.* **2001**, *46*, 1836–1843. [[CrossRef](#)]
34. Del Castillo, C.E.; Coble, P.G.; Morell, J.M.; López, J.M.; Corredor, J.E. Analysis of the optical properties of the Orinoco River plume by absorption and fluorescence spectroscopy. *Mar. Chem.* **1999**, *66*, 35–51. [[CrossRef](#)]
35. Cory, R.M.; McKnight, D.M. Fluorescence Spectroscopy Reveals Ubiquitous Presence of Oxidized and Reduced Quinones in Dissolved Organic Matter. *Environ. Sci. Technol.* **2005**, *39*, 8142–8149. [[CrossRef](#)] [[PubMed](#)]
36. Murphy, K.R.; Ruiz, G.M.; Dunsmuir, W.T.M.; Waite, T.D. Optimized Parameters for Fluorescence-Based Verification of Ballast Water Exchange by Ships. *Environ. Sci. Technol.* **2006**, *40*, 2357–2362. [[CrossRef](#)] [[PubMed](#)]
37. Chen, W.; Westerhoff, P.; Leenheer, J.A.; Booksh, K. Fluorescence Excitation–Emission Matrix Regional Integration to Quantify Spectra for Dissolved Organic Matter. *Environ. Sci. Technol.* **2003**, *37*, 5701–5710. [[CrossRef](#)]
38. Stedmon, C.A.; Markager, S. Resolving the variability in dissolved organic matter fluorescence in a temperate estuary and its catchment using PARAFAC analysis. *Limnol. Oceanogr.* **2005**, *50*, 686–697. [[CrossRef](#)]
39. Leenheer, J.A.; Croué, J.P. Peer reviewed: Characterizing aquatic dissolved organic matter. *Environ. Sci. Technol.* **2003**, *37*, 18A–26A. [[CrossRef](#)]
40. Coble, P.G.; Del Castillo, C.E.; Avril, B. Distribution and optical properties of CDOM in the Arabian Sea during the 1995 Southwest Monsoon. *Deep Sea Res. Part II Top. Stud. Oceanogr.* **1998**, *45*, 2195–2223. [[CrossRef](#)]
41. Dosskey, M.G.; Bertsch, P.M. Transport of Dissolved Organic Matter through a Sandy Forest Soil. *Soil Sci. Soc. Am. J.* **1997**, *61*, 920–927. [[CrossRef](#)]
42. Fu, Q.L.; He, J.Z.; Blaney, L.; Zhou, D.M. Roxarsone binding to soil-derived dissolved organic matter: Insights from multi-spectroscopic techniques. *Chemosphere* **2016**, *155*, 225–233. [[CrossRef](#)]
43. Dandajeh, H.A.; Ladommatos, N.; Hellier, P.; Eveleigh, A. Effects of unsaturation of C2 and C3 hydrocarbons on the formation of PAHs and on the toxicity of soot particles. *Fuel* **2017**, *194*, 306–320. [[CrossRef](#)]
44. Ye, H.; Liu, B.; Wang, Q.; How, Z.T.; Zhan, Y.; Chelme-Ayala, P.; Guo, S.; Gamal El-Din, M.; Chen, C. Comprehensive chemical analysis and characterization of heavy oil electric desalting wastewaters in petroleum refineries. *Sci. Total Environ.* **2020**, *724*, 138117. [[CrossRef](#)] [[PubMed](#)]
45. Zhou, Q.Q.; Su, R.G.; Bai, Y.; Zhang, C.S.; Shi, X.Y. Characterization of Chromophoric dissolved organic matter (CDOM) in Zhoushan fishery using excitation-emission matrix spectroscopy (EEMs) and parallel factor analysis (PARAFAC). *Estuar. Coast.* **2017**, *40*, 1325–1345. [[CrossRef](#)]
46. Bao, Y.; Niu, J.; Xu, Z.; Gao, D.; Shi, J.; Sun, X.; Huang, Q. Removal of perfluorooctane sulfonate (PFOS) and perfluorooctanoate (PFOA) from water by coagulation: Mechanisms and influencing factors. *J. Colloid Interface Sci.* **2014**, *434*, 59–64. [[CrossRef](#)] [[PubMed](#)]
47. Zhai, L.Z.; Sun, Y.H.; He, C. Research on coagulation/sedimentation process for simulation of fluorine-containing wastewater treatment. *Appl Mech Mater* **2013**, *361*, 755–759. [[CrossRef](#)]
48. Pan, Z. The Study of oil Pollution Recognition Measurement Method and Experiment Based on Fluorescence Spectrum Analysis. Ph.D. Dissertation, Yanshan University, Qinhuangdao, China, 2012.
49. Sulzberger, B.; Durisch Kaiser, E. Chemical characterization of dissolved organic matter (DOM): A prerequisite for understanding UV-induced changes of DOM absorption properties and bioavailability. *Aquat. Sci.* **2009**, *71*, 104–126. [[CrossRef](#)]
50. Balch, J.; Guéguen, C. Effects of molecular weight on the diffusion coefficient of aquatic dissolved organic matter and humic substances. *Chemosphere* **2015**, *119*, 498–503. [[CrossRef](#)]
51. Shin, Y.; Lee, E.J.; Jeon, Y.J.; Hur, J.; Oh, N.H. Hydrological changes of DOM composition and biodegradability of rivers in temperate monsoon climates. *J. Hydrol.* **2016**, *540*, 538–548. [[CrossRef](#)]
52. Liu, S.; Zhu, Y.; Liu, L.; He, Z.; Giesy, J.P.; Bai, Y.; Sun, F.; Wu, F. Cation-induced coagulation of aquatic plant-derived dissolved organic matter: Investigation by EEM-PARAFAC and FT-IR spectroscopy. *Environ. Pollut.* **2018**, *234*, 726–734. [[CrossRef](#)]
53. Zhou, Y.; Xie, Y.; Wang, M.; Zou, F.; Zhang, C.; Guan, Z.; Yan, M. In-situ characterization of dissolved organic matter removal by coagulation using differential UV–Visible absorbance spectroscopy. *Chemosphere* **2020**, *242*, 125062. [[CrossRef](#)] [[PubMed](#)]
54. Zhu, G.; Bian, Y.; Hursthouse, A.S.; Xu, S.; Xiong, N.; Wan, P. The role of magnetic MOFs nanoparticles in enhanced iron coagulation of aquatic dissolved organic matter. *Chemosphere* **2020**, *247*, 125921. [[CrossRef](#)] [[PubMed](#)]
55. Huang, M.; Song, Q.; Xing, X.; Jian, W.J.; Liu, Y.; Zhao, Z.L. Analysis of fluorescence spectrum characteristics of petroleum polluted water. *Spectrosc. Spectr. Anal.* **2014**, *34*, 2466–2471. [[CrossRef](#)]
56. Yang, C.; Zhong, N.; Shi, Y.; Wang, F.; Chen, D. Three-dimensional fluorescence spectrum characteristics of dissolved organic matter in coal mine area. *Spectrosc. Spectr. Anal.* **2008**, *28*, 174–177.
57. Yang, S.; Wang, F.; Tang, Q.; Wang, P.; Xu, Z.; Liang, J. Utilization of ultra-light carbon foams for the purification of emulsified oil wastewater and their adsorption kinetics. *Chem. Phys.* **2019**, *516*, 139–146. [[CrossRef](#)]

58. Dotson, A.; Westerhoff, P. Occurrence and removal of amino acids during drinking water treatment. *J. Am. WATER Work. Assoc.* **2009**, *101*, 101–115. [[CrossRef](#)]
59. Zhou, Y.; Jeppesen, E.; Zhang, Y.; Shi, K.; Liu, X.; Zhu, G. Dissolved organic matter fluorescence at wavelength 275/342 nm as a key indicator for detection of point-source contamination in a large Chinese drinking water lake. *Chemosphere* **2016**, *144*, 503–509. [[CrossRef](#)]
60. Fang, H. Study on biological stability of drinking water and removing organic matter by water purification processes. Ph.D. Dissertation, Southeast University, Nanjing, China, 2006.
61. Lou, J.C.; Chen, B.H.; Chang, T.W.; Yang, H.W.; Han, J.Y. Variation and removal efficiency of assimilable organic carbon (AOC) in an advanced water treatment system. *Environ. Monit. Assess.* **2011**, *178*, 73–83. [[CrossRef](#)]
62. Soonglerdsongpha, S.; Kasuga, I.; Kurisu, F.; Furumai, H. Comparison of assimilable organic carbon removal and bacterial community structures in biological activated carbon process for advanced drinking water treatment plants. *Sustain. Environ. Res.* **2011**, *21*, 59–64.
63. Zhao, C.; Lin, D.; Wang, Z. Researching Progress of Micro-electrolysis Technology. *Environ. Protec. Oil Gas Fields* **2013**, *23*, 59–61. [[CrossRef](#)]
64. Huang, J.G.; Zhong, L. Experimental study on pretreatment of oil refining wastewater by waste ferric/active carbon micro-electrolysis process. *Sci. Technol. Chem. Indus.* **2010**, *5*, 10–14. [[CrossRef](#)]
65. Ma, S.; Wu, N.; Ma, Q.; Li, F.; Yang, J.; Li, D.; Li, J. Treatment of Oily Wastewater with Iron-Carbon Internal Electrolysis Process Enhanced by Ultrasonic. *Adv. Sci. Lett.* **2013**, *19*, 1869–1872. [[CrossRef](#)]
66. Tomaszewska, M.; Mozia, S. Removal of organic matter from water by PAC/UF system. *Water Res.* **2002**, *36*, 4137–4143. [[CrossRef](#)]
67. Jin, P.; Jin, X.; Bjerkelund, V.A.; Østerhus, S.W.; Wang, X.C.; Yang, L. A study on the reactivity characteristics of dissolved effluent organic matter (EfOM) from municipal wastewater treatment plant during ozonation. *Water Res.* **2016**, *88*, 643–652. [[CrossRef](#)] [[PubMed](#)]